JARO 15: 739–754 (2014)
DOI: 10.1007/s10162-014-0479-3

JARO
Journal of the Association for Research in Otolaryngology

Research Article

Distribution of Na,K-ATPase α Subunits in Rat Vestibular Sensory Epithelia

Olga Schuth,[1] Will J. McLean,[2] Ruth Anne Eatock,[3] and Sonja J. Pyott[1,4]

[1]*Department of Biology and Marine Biology, University of North Carolina Wilmington, 601 South College Road, Wilmington, NC 28403, USA*

[2]*Eaton-Peabody Laboratories, Massachusetts Eye and Ear Infirmary, 243 Charles Street, Boston, MA 02114, USA*

[3]*Department of Neurobiology, University of Chicago, Chicago, IL 60637, USA*

[4]*Present Address: Department of Otorhinolaryngology, Head & Neck Surgery University Medical Center Groningen, University of Groningen, P.O. Box 30001, Groningen, RB 9700, The Netherlands*

Received: 23 January 2014; Accepted: 1 July 2014; Online publication: 5 August 2014

ABSTRACT

The afferent encoding of vestibular stimuli depends on molecular mechanisms that regulate membrane potential, concentration gradients, and ion and neurotransmitter clearance at both afferent and efferent relays. In many cell types, the Na,K-ATPase (NKA) is essential for establishing hyperpolarized membrane potentials and mediating both primary and secondary active transport required for ion and neurotransmitter clearance. In vestibular sensory epithelia, a calyx nerve ending envelopes each type I hair cell, isolating it over most of its surface from support cells and posing special challenges for ion and neurotransmitter clearance. We used immunofluorescence and high-resolution confocal microscopy to examine the cellular and subcellular patterns of NKAα subunit expression within the sensory epithelia of semicircular canals as well as an otolith organ (the utricle). Results were similar for both kinds of vestibular organ. The neuronal NKAα3 subunit was detected in all afferent endings—both the calyx afferent endings on type I hair cells and bouton afferent endings on type II hair cells—but was not detected in efferent terminals. In contrast to previous results in the cochlea, the NKAα1 subunit was detected in hair cells (both type I and type II) but not in supporting cells. The expression of distinct NKAα subunits by vestibular hair cells and their afferent endings may be needed to support and shape the high rates of glutamatergic neurotransmission and spike initiation at the unusual type I-calyx synapse.

Keywords: vestibular hair cells, calyx terminals, Na,K-ATPase

Correspondence to: Sonja J. Pyott · Department of Biology and Marine Biology · University of North Carolina Wilmington · 601 South College Road, Wilmington, NC 28403, USA. Telephone: +1-910-9622323; email: pyotts@uncw.edu

INTRODUCTION

Afferent signaling in the vestibular sensory epithelia of mammals and other amniotes relies on primary afferents that are classified by their terminal morphology as pure calyx afferents, which ensheath flask-shaped type I vestibular hair cells, pure bouton afferents, which contact columnar-shaped type II vestibular hair cells, and dimorphic afferents, which form both calyx and bouton terminals on both vestibular hair cell types (Fernandez et al. 1988; Fernandez et al. 1990). To relay afferent signals, both calyx and bouton endings must possess molecular mechanisms that support glutamatergic synaptic transmission, including mechanisms to establish appropriate concentration gradients, maintain hyperpolarized membrane potentials, and control the clearance of glutamate from the synaptic cleft. The unique morphology of vestibular calyces, postsynaptic structures that almost completely surround the type I hair cells, poses additional challenges to ensure the clearance of K^+ ions and glutamate that would be expected to accumulate rapidly within the enclosed space between

the type I hair cell and calyx ending, especially given the high rates of afferent transmission (reviewed in Eatock and Songer 2011). The molecular mechanisms that regulate concentration gradients, membrane potential, as well as ion and neurotransmitter clearance at both afferent and efferent contacts undoubtedly have important implications for the encoding of vestibular stimuli.

In other excitable and non-excitable cells, the Na,K-ATPase (NKA) is essential for establishing and maintaining hyperpolarized membrane potentials and clearing ions and neurotransmitters both directly by mediating primary active transport (transport mediated by transmembrane ATPases) and indirectly by supporting secondary active transport (transport mediated by coupled transporters which depend on the concentration gradients established by primary active transport). The NKA is a membrane-bound protein that uses the energy from adenosine triphosphate (ATP) hydrolysis to export three Na^+ ions for every two K^+ ions imported. The NKAα subunits contain the residues necessary for ATP hydrolysis and ion transport. The diversity of α (1–4) and also accessory β (1–3), and regulatory FXYD (1–7) subunits allows NKA transport properties, such as Na^+ and ATP affinities and voltage-dependent pumping efficiencies, to be tailored to specific cellular demands (Geering 2008).

Although the contribution of the NKAα subunit to the establishment of the endolymphatic potential is well recognized (Wangemann 2002), its contribution more directly to afferent signaling is less clear but nevertheless suggested by earlier work reporting the presence of NKAα subunits specifically within the nerve endings of the vestibular sensory epithelia (Spicer et al. 1990; Ichimiya et al. 1994; McGuirt and Schulte 1994; Schulte and Steel 1994; ten Cate et al. 1994). More recent immunofluorescent examination of the expression of NKAα subunits in the auditory sensory epithelium (McLean et al. 2009), which revealed distinct distributions of the NKAα1 and α3 subunits, together with the recent identification of molecular microdomains, or subcellular regions of restricted protein expression, within calyx endings (Lysakowski et al. 2011), suggest that NKAα subunits may be distributed not only in specific cell types within the vestibular sensory epithlelia but also within specific regions of the calyx ending.

These previous observations and the unique morphology and physiology of vestibular afferent terminals motivated our examination of the cellular and subcellular patterns of NKAα subunit expression within the sensory epithelia of the utricle (the utricular macula) and the horizontal and anterior canals (the semicircular canal cristae). Isolation of both otolithic and canal endorgans allowed comparison of NKAα expression differences in the structures responsible for encoding linear acceleration compared with rotational movements and also permitted both cross-sectional and profile views of the sensory hair cells and their afferent and efferent terminals.

METHODS

Immunofluorescence

In accordance with animal protocols approved by the University of North Carolina Wilmington Animal Care and Use Committee, Sprague Dawley rats (Charles River Laboratories), aged between 17 and 25 days or as otherwise indicated in the text, were deeply anesthetized by isoflurane inhalation and then decapitated. The isolated temporal bones were transferred to ice-cold phosphate-buffered saline (PBS) and the bony labyrinths removed and placed into fresh PBS. To examine both otolith and canal endorgans, we excised the part of the membranous labyrinth housing the sensory epithelia of the utricle (the utricular macula) and the horizontal and anterior canals (the semicircular canal cristae). The membranous labyrinth was then opened to allow removal of the utricular otoliths. Preparations were transferred to ice-cold 4 % paraformaldehyde in PBS, fixed for 30 min to 3 h depending on the primary antibody used. In particular, immunofluorescent detection using the monoclonal antibody against the NKAα3 is enhanced with longer fixation times (our observation as well as a personal communication from Dr. Douglas Fambrough). In contrast, in our experience, most other antibodies, notably the polyclonal antibody against the GluA2/3, require shorter fixation times (1 h or less). Therefore, fixation times often varied in order to optimize immunofluorescence detection depending on the primary antibodies used. Following incubation in the primary antibodies, preparations were rinsed three times, 10 min each in PBS. For immunofluorescent staining, preparations were incubated in blocking buffer (PBS with either 5 % normal goat serum or 1 % bovine serum albumin, 4 % Triton X-100, and 1 % saponin) for 1 to 2 h, incubated in the primary antibody diluted 1:50 to 1:300 in blocking buffer overnight, washed three times, 10 min each in PBS with 0.2 % Triton X-100 (PBT), incubated in the appropriate secondary antibody diluted 1:500 in blocking buffer for 2 h, washed again three times, 10 min each in PBT, washed one time, 10 min each in PBS, and then mounted in Vectashield (Vector Labs). The use of blocking buffer containing a relatively high percentage of Triton X-100 (4 %) is necessary for immunofluorescent staining of some antibodies, notably those against calretinin (our observation as well as a personal communication from Dr. Florin Vranceanu), and therefore, is used routinely in our protocols. All incubation and rinses were performed on a rocking table at room temperature.

The primary antibodies used in this study are summarized in Table 1 and were chosen because their specificity has been established (see references in Table 1) and because they were used previously to characterize NKAα subunit distribution in the auditory sensory epithelium (McLean et al. 2009). In all cases, experiments performed in the absence of primary antibody showed no immunoreactivity. Patterns of immunoreactivity were confirmed in a minimum of four independent experiments. Secondary antibodies were purchased from Molecular Probes (Life Technologies): Alexa Fluor 488 Donkey Anti-Mouse IgG (A21202), Alexa Fluor 594 Donkey Anti-Goat IgG (A11058), Alexa Fluor 488 Goat Anti-Mouse IgG (A11029), Alexa Fluor 594 Goat Anti-Rabbit IgG (A11037), Alexa Fluor 488 Goat Anti-Mouse IgG1 (A21121), Alexa Fluor 568 Goat Anti-Rabbit IgG (A11011), and Alexa Fluor 647 Goat Anti-Mouse IgG2A (A21241).

Microscopy

Fluorescence images were acquired using an Olympus Fluoview FV1000 confocal microscope with either a 20× Olympus UPlanSApo lens (N. A. 0.75) or 60×

TABLE 1
Primary antibodies used in the study

Antibody	*Immunogen*	*Supplier*	*Host*	*Specificity*
Na,K-ATPase α3 (NKAα3)	Amino terminus of the canine NKAα3	Pierce antibodies (MA3-915)	Mouse monoclonal (IgG1)	Western blotting of canine skeletal muscle extract and immunohistochemical staining of rat retina
Na,K-ATPase α3 (NKAα3)	Peptide mapping to an internal region of the human NKAα3 (between amino acids 400 and 450 of protein accession number P13637)	Santa Cruz Biotechnology (sc-16,052)	Goat polyclonal	Western blotting of rat brain extracts
Myosin VI (Myo6)	Synthetic peptide corresponding to the carboxy terminus of the human Myo6	Sigma (M5187)	Rabbit polyclonal	Western blotting of whole extract of dog MDCK kidney cells and immunofluorescent staining of rat NRK kidney cells
Type III β-tubulin (TuJ)	Purified rat brain microtubules	Covance (MMS-435P)	Mouse monoclonal (IgG2A)	Western blotting of rat brain and immunofluorescent staining of rat hippocampus
Calretinin	Recombinant at calretinin	Millipore (AB5054)	Rabbit polyclonal	Immunohistochemical staining of rat brain cortex
K_V7.4	Synthetic peptide, corresponding to the carboxy terminus of the human and mouse K_V7.4 protein	Kindly donated by Dr. Bechara Kachar (PB180)	Rabbit polyclonal	(Beisel et al. 2005)
Synapsin	Synapsin I purified from bovine brain	Millipore (AB1543P)	Rabbit polyclonal	Immunohistochemical staining of hippocampal neurons
Excitatory amino acid transporter 5 (EAAT5)	Synthetic peptide corresponding to the human EAAT5	Santa Cruz Biotechnology (sc-18,779)	Goat polyclonal	(See Dalet et al. 2012)
Glutamate receptor 2/3 (GluA2/3)	Synthetic peptide corresponding to the carboxy terminus of the rat GluR2	Chemicon/ Millipore (AB1506)	Rabbit polyclonal	Western blotting of rat brain lysate
Na,K-ATPase α1 (NKAα1)	NKAα purified from rabbit kidney	Santa Cruz Biotechnology (sc-21,712)	Mouse monoclonal (IgG1)	Western blot analysis of rat brain microsomes
Na,K-ATPase α1 (NKAα1)	NKAα purified from chicken kidney	Developmental Studies Hybridoma Bank (α6F)	Mouse monoclonal (IgG1)	(Arystarkhova and Sweadner 1996)
Na,K-ATPase α2 (NKAα2)	Synthetic peptide corresponding to an internal region of the human NKAα2	Santa Cruz Biotechnology (sc-16,049)	Goat polyclonal	Immunohistochemical staining of human colon tumor
Na,K-ATPase α2 (NKAα2)	Synthetic peptide corresponding to the rat NKAα2	Generously provided by Dr. Thomas Pressley (Anti-HERED)	Rabbit polyclonal	(Pressley 1992)

Olympus PlanoApo oil immersion lens (N. A. 1.42) under the control of the Olympus Fluoview FV1000 version 2.1 software. Z-stacks through the preparation were collected in 0.44 μm steps. The step size (optical section thickness) was determined to be half the distance of the theoretical *z*-axis resolution (the Nyquist sampling frequency). Images were acquired in a 1,024×1,024 raster ($x=y=0.207$ μm/pixel at 60×) at sub-saturating laser intensities for each channel. Images were viewed in the Imaris 6.4 three-dimensional (3D) image visualization and analysis software (Bitplane Inc.) and are presented as either z-projections through a subset of the collected optical stack or as a single optical section.

RESULTS

The NKAα3 Subunit Is Expressed in the Vestibular Sensory Epithelia

We first examined the distribution of the neuronal NKAα3 subunit in preparations of the utricular macula and anterior and horizontal cristae excised from rats aged P17 to P25. To confirm the pattern and specificity of immunoreactivity, we double-immunolabeled preparations with a monoclonal antibody against NKAα3 (red, Fig. 1) and a goat polyclonal antibody (green, Fig. 1) against NKAα3. Projections through a z-stack of optical sections taken at low magnification and spanning the entire preparation show that both antibodies abundantly label both the utricular and canal sensory epithelia (Fig. 1A, B) and that the immunolabel colocalizes (Fig. 1C). To examine the cellular pattern of NKAα3 immunoreactivity, we viewed the central region of the horizontal crista (Fig. 1D–F) and the comparable striolar region of the utricular macula (Fig. 1G–I) under high magnification. Preparations of the crista were transverse to the long axis of the organ, exposing the sensory cells and their neuronal terminals in profile. High magnification projections through a z-stack of confocal sections spanning a single layer of sensory cells reveal colocalized NKAα3 immunoreactivity for the monoclonal (Fig. 1D, F) and polyclonal (Fig. 1E, F) in neuronal terminals contacting and, in some cases, surrounding the hair cells, presumptive bouton and calyx endings. Preparations of the utricular macula were parallel to the surface of the macula, providing cross-sectional views of the sensory cells and their neuronal terminals. High-magnification single optical sections reveal colocalized NKAα3 immunoreactivity for the monoclonal (Fig. 1G, I) and polyclonal (Fig. 1H, I) antibodies in the calyx endings. The colocalization of label for NKAα3 monoclonal and polyclonal antibodies in cell membranes suggests that the immunolabel is specific for the NKAα3 subunit. Small differences in the staining intensity between the two antibodies may reflect differences in the epitopes as well as differences in the optimal fixation conditions for each antibody.

To examine whether sensory hair cell membranes are immunoreactive for NKAα3, we labeled preparations with the monoclonal antibody against NKAα3 (green, Fig. 2) and a polyclonal antibody against the hair cell marker Myosin VI (Myo6, red, Fig. 2), an unconventional myosin enriched in auditory and vestibular hair cells (Hasson et al. 1997). In the central region of the horizontal crista, projections through a z-stack of confocal sections spanning a single layer of sensory hair cells reveal NKAα3 immunoreactivity (Fig. 2A) surrounding type I hair cells identified morphologically by their more constricted necks (Fig. 2B, C). Like the calyx endings around type I hair cells, NKAα3 immunoreactivity terminates at the necks of the hair cells (Fig. 2C), below the apical surface, suggesting NKAα3 immunoreactivity is associated with the membrane of the calyx endings and not the hair cells. In contrast to the type I hair cells, morphologically identified type II hair cells are not enveloped by NKAα3 immunoreactivity but instead are contacted by NKAα3-positive bouton endings that may be either afferent or efferent terminals (Fig. 2C). Consistent with NKAα3 expression in calyx and bouton endings, single optical sections from the striolar region of the utricle show NKAα3 immunoreactivity (Fig. 2D, F) in the calyces that completely surrounds type I hair cells (Fig. 2D, E) as well as in bouton endings on type II hair cells (Fig. 2F, G). Where clearly resolved, the inner (open arrowhead) and outer (closed arrowhead) calyx membranes have been labeled (Fig. 2D).

The NKAα3 Subunit Is Expressed in Both Calyx and Bouton Afferent Endings

To examine expression of the NKAα3 subunit within the afferent endings on the sensory hair cells, we triple immunolabeled preparations with the monoclonal (IgG1) antibody against NKAα3 (green, Fig. 3), the polyclonal antibody against the hair cell marker Myosin VI (Myo6, red, Fig. 3), and a monoclonal (IgG2A) antibody against the type III β-tubulin (TuJ, blue, Fig. 3), a β-tubulin isotype expressed within vestibular afferent calyx and bouton endings (Perry et al. 2003). In the central region of the horizontal crista, projections through a z-stack of confocal sections spanning a single layer of sensory hair cells reveal NKAα3 immunoreactivity (Fig. 3A) in the calyx and bouton terminals of TuJ-positive fibers (Fig. 3B). Myo6 immunoreactivity clearly shows that the hair cells extend apically beyond the limit of NKAα3 immuno-

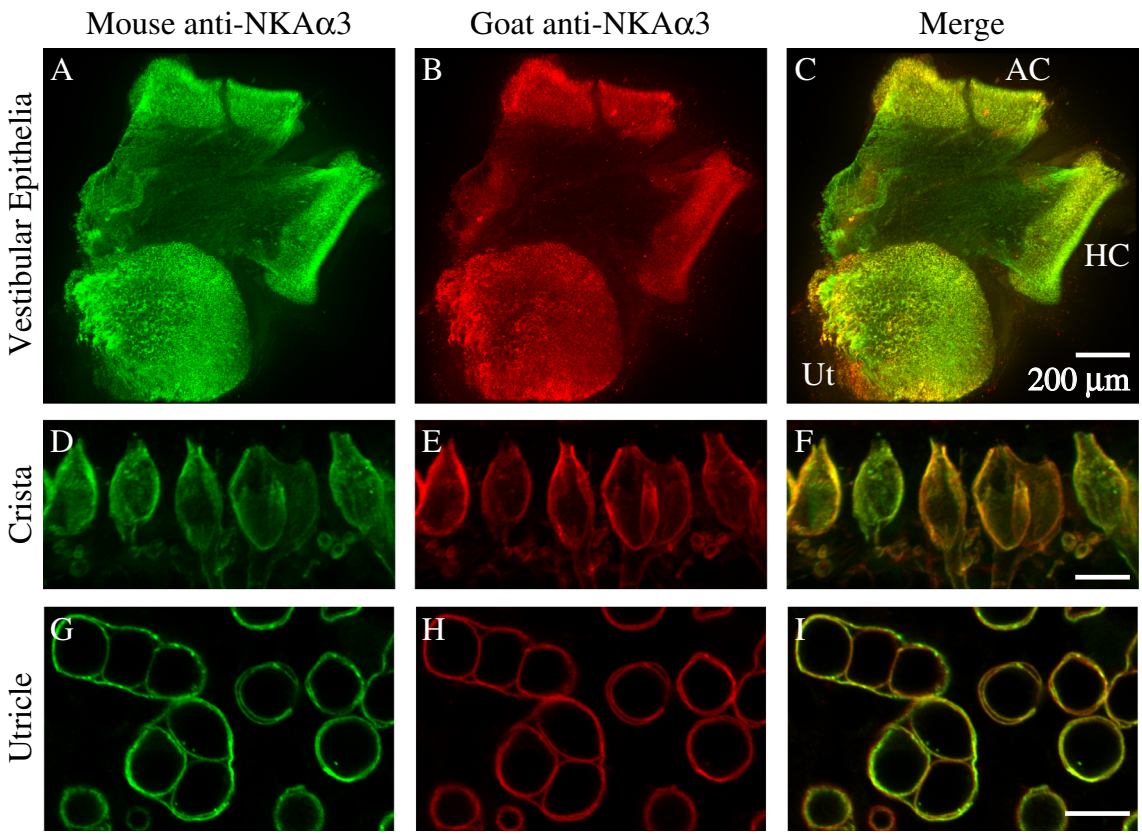

FIG. 1. NKAα3 is present in the vestibular sensory epithelia. **A–C** Projections through a z-stack of confocal sections taken at low magnification and spanning the entire preparation of the vestibular sensory epithelia containing the utricle (Ut), anterior crista (AC), and horizontal crista (HC) double-immunolabeled with a mouse monoclonal anti-NKAα3 (*green*, **A**) and goat polyclonal anti-NKAα3 (*red*, **B**) show colocalized immunoreactivity (*merge*, **C**) in the sensory epithelia. **D–F** Projections through a z-stack of confocal sections taken at high magnification and spanning a narrow region of the central region of the horizontal crista also double-immunolabeled with a mouse monoclonal anti-NKAα3 (*green*, **D**) and goat polyclonal anti-NKAα3 (*red*, **E**) show colocalized immunoreactivity in neuronal terminals approaching and in some cases surrounding the hair cells (*merge*, **F**). **G–I** Single optical sections taken at high magnification of the striolar region of the utricle reveal NKAα3 immunoreactivity for both the mouse monoclonal anti-NKAα3 (*green*, **G**) and goat polyclonal anti-NKAα3 (*red*, **H**), colocalized in simple and complex calyces, viewed in cross-section (*merge*, **I**). (Simple and complex calyces surround single and multiple type I hair cells, respectively. Two complex calyces around three hair cells each are visible in the left half of this field, with the remaining circular profiles corresponding to simple calyces.) Similar colocalization was observed in high magnification views of the anterior crista (data not shown). Scale *bars* measure 10 µm, unless otherwise indicated.

reactivity (Fig. 3C), consistent with NKAα3 expression in the afferent terminals but not the hair cells. Figure 3D–F show higher magnifications of representative bouton endings (Fig. 3D), simple calyces (Fig. 3E), and complex calyces (Fig. 3F). In all cases, NKAα3 immunoreactivity completely envelopes the TuJ staining of afferent fibers and endings; where indicated, the inner calyx membrane (open arrowhead) and outer calyx membrane (closed arrowhead) are clearly resolved (Fig. 3E, F). This relative localization within the calyx terminal is expected for membrane-associated NKAα3 and cytosolic TuJ. Expression in the vestibular ganglion cells was not examined. The calyx terminals are unambiguously afferent, but bouton terminals could in principle be either afferent or efferent, since previous reports did not report whether vestibular efferent fibers are TuJ-positive (Perry et al. 2003). As shown later, however, immunoreactivity for synapsin suggests that efferent terminals are TuJ-negative.

We additionally investigated whether there was a difference between afferent types by double immunolabeling with an antibody for calretinin; in the central and striolar zones of vestibular epithelia, calretinin-positive afferents are pure-calyx afferents, while calretinin-negative afferents are dimorphic (Desmadryl and Dechesne 1992; Leonard and Kevetter 2002; Desai et al. 2005b; Desai et al. 2005a). We observed NKAα3-immunoreactivity in both calretinin-positive and calretinin-negative TuJ-positive

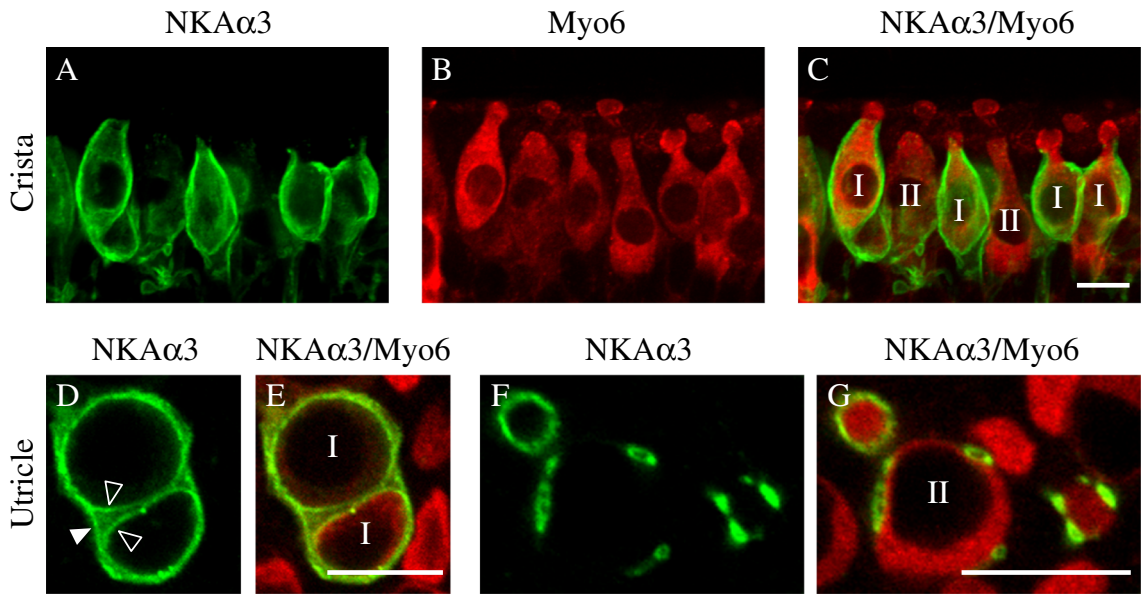

FIG. 2. NKAα3 is localized in afferent endings of both type I and II vestibular hair cells. **A–C** Projections through a z-stack of confocal sections taken at high magnification and spanning a narrow region of the central zone of the horizontal crista, double-immunolabeled with a mouse monoclonal anti-NKAα3 (*green*, **A**) and rabbit polyclonal anti-Myo6 (*red*, **B**), show NKAα3 immunoreactivity in neuronal endings approaching and in some cases surrounding the Myo6-positive hair cells (*merge*, **C**). **D–G** Single optical sections taken at high magnification of the striolar region of the utricle reveal NKAα3 immunoreactivity in afferent calyces (*green*, **D** and **F**) that completely surround Myo6-positive type I hair cells (*red*, **E**) or in the membranes of neuronal terminals contacting Myo6-positive type II hair cells (*red*, **G**). Type I and II hair cells are labeled 1 and II (**C**, **E**, **G**). In **D**, the inner-face membrane of the calyx (*open arrowhead*) can be distinguished from the outer-face calyx membrane (*closed arrowhead*). Similar patterns of immunoreactivity were observed in high magnification views of the anterior crista (data not shown). Scale *bars* measure 10 μm.

afferent calyces (data not shown), suggesting that NKAα3 is present in both pure-calyx afferents and the larger population of dimorphic afferents.

The NKAα3 Subunit Is Expressed Throughout Each Calyx Terminal and in All Zones of the Sensory Epithelia

NKAα3 immunoreactivity in calyx endings is clearly visible in the outer membrane and also appears to be present in the inner face adjacent to the type I hair cell. To localize NKAα3 immunoreactivity to particular molecular microdomains of the calyx (Lysakowski et al. 2011), we double immunolabeled preparations with a monoclonal antibody against NKAα3 (green, Fig. 4) and a polyclonal antibody against $K_V7.4$ (red, Fig. 4), a voltage-gated K^+ channel subunit enriched within Domain 1 of the calyx inner face. In the central region of the horizontal crista, projections through a z-stack of confocal sections spanning a single layer of sensory hair cells reveal NKAα3 immunoreactivity (Fig. 4A, C) that colocalizes with $K_V7.4$ immunoreactivity in Domain 1, the calyx inner face, but also extends into the $K_V7.4$-negative calyx domains, including Domain 2, the apical domain, and Domain 3, the calyx outer face (Fig. 4B, C). Higher magnifications of the calyces boxed in Figure 4C clearly show NKAα3 immunoreactivity throughout the calyx terminal, including the $K_V7.4$-positive Domain 1 (open arrowhead) as well as the calyx outer membrane (closed arrowhead, Fig. 4G). Consistent with NKAα3 expression in both the calyx outer membrane and $K_V7.4$-positive Domain 1, single optical sections from the striolar region of the utricle show NKAα3 immunoreactivity in both the calyx outer membrane (closed arrowhead) as well as colocalized with the $K_V7.4$-positive calyx inner face (open arrowhead, Fig. 4D–F and H). Given that $K_V7.4$ is not expressed by type I hair cells in rat (Hurley et al. 2006) or adult mouse (Spitzmaul et al. 2013), colocalization of $K_V7.4$ and NKAα3 immunoreactivity further indicates that NKAα3 is expressed in the calyx endings but not in the type I hair cells. Similarly, the NKAα3 immunoreactivity in the vicinity of type II hair cells is limited to and continuous with bouton endings on the hair cells, consistent with the interpretation that NKAα3 is also absent from type II hair cell membranes. NKAα3 immunoreactivity was intense in the calyx inner and outer face, in both the crista and utricle, except in regions enriched with $K_V7.4$ (as seen in Fig. 4H);

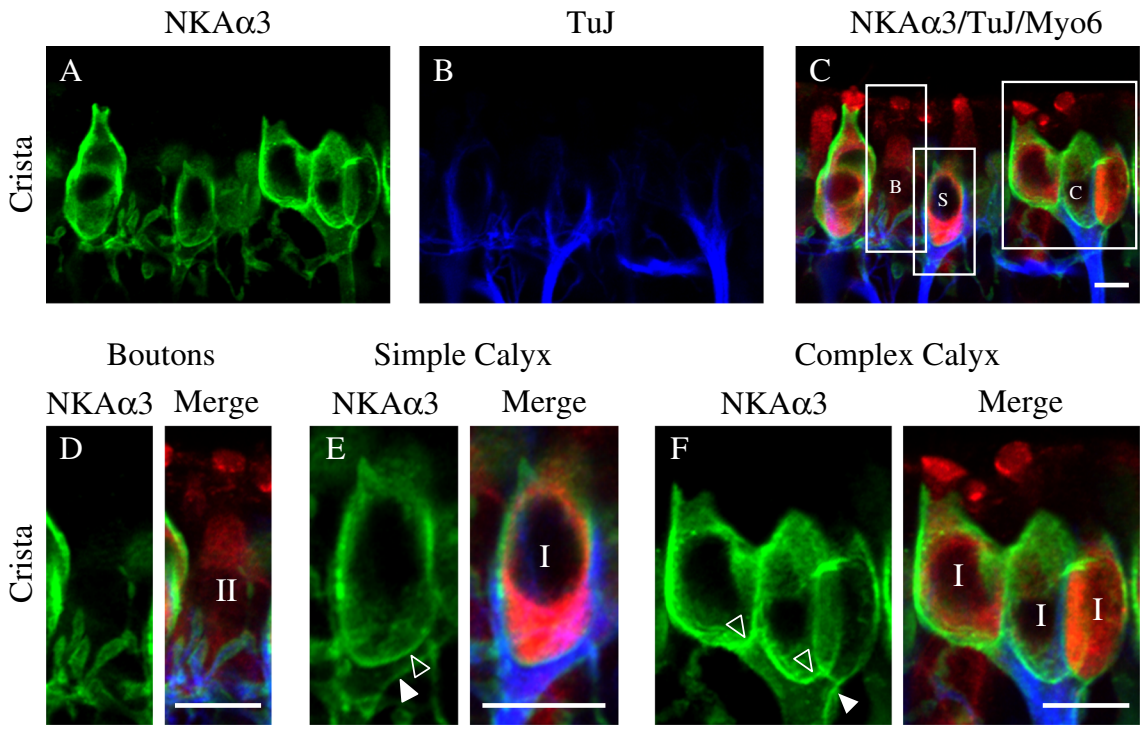

FIG. 3. NKAα3 is expressed in both calyx and bouton afferent endings. **A–C** High magnification micrographs of the central region of the horizontal crista triple-immunolabeled with a mouse monoclonal (IgG1) anti-NKAα3 (*green*, **A**), mouse monoclonal (IgG2A) anti-TuJ (*blue*, **B**), and a rabbit polyclonal anti-Myo6 (*red*, **C**). NKAα3 immunoreactivity was associated with TuJ-identified bouton terminals (labeled *B*) on type II hair cells as well as simple (labeled *S*) and complex (labeled *C*) calyx terminals around Myo6-positive type I hair cells (*merge*, **C**). **D** Higher magnification views of bouton afferents also show NKAα3 immunoreactivity (*green*) in the membranes of TuJ-positive (*blue*) boutons and identify the Myo6-positive (*red*) hair cells as type II. **E–F** Higher magnification views of simple (**E**) and complex (**F**) calyx terminals show NKAα3 immunoreactivity (*green*) that completely surrounds TuJ-positive (*blue*) calyces and identifies the Myo6-positive (*red*) hair cells as type I. Where clearly resolved, the inner-face (*open arrowhead*) and outer-face (*closed arrowhead*) calyx membranes are indicated (**D**, **E**). Across samples, NKAα3 immunoreactivity appeared more intense in complex calyces compared with either simple or bouton calyces (as appreciated in Fig. 3A). Micrographs represent projections through the minimal number of optical sections required to completely visualize the hair cells and their afferent terminals. Similar patterns of immunoreactivity were observed in high magnification views of the anterior crista and utricle (data not shown). Scale *bars* measure 10 μm.

conceivably, localized enrichment of $K_V7.4$ results in a localized reduction in NKAα3 as these membrane proteins compete for space.

In addition to localizing the NKAα3 subunit within calyx microdomains, double-immunolabeling with $K_V7.4$ antibody also allowed examination of regional differences in the distribution of NKAα3 within the sensory epithelia. Whereas $K_V7.4$ immunoreactivity is topographically enriched in the central and striolar regions of the vestibular sensory epithelia (Rocha-Sanchez et al. 2007), projections through a z-stack of optical sections taken at low magnification and spanning the entire anterior crista (Fig. 5A–C), horizontal crista (not shown), and utricle (Fig. 5D–F) reveal NKAα3 immunoreactivity throughout the vestibular sensory epithelia. Zonal differences in the apparent intensity of immunostaining may reflect zonal differences in morphology: Less intense NKAα3 immunoreactivity in the utricular striola likely reflects the fact that striolar hair cells are larger and less densely packed (reviewed in Eatock and Songer 2011). Individual complex calyces in the striola do show more intense NKAα3 immunoreactivity compared with calyces outside the striola.

The NKAα3 Subunit Colocalizes with Glutamate Transporters and Receptors on Calyx Afferent Terminals

Because Na^+ concentration gradients are essential to the functioning of glutamate receptors and transporters, both key components of glutamatergic transmission, we also examined the relative localization of the NKAα3 subunit and glutamate receptors (specifically subtypes GluA2/3, Fig. 6A–C), as well as the glutamate transporter EAAT5 (Fig. 6D–F), recently localized to the calyx afferent terminal (Dalet et al. 2012). We specifically examined afferent calyces in

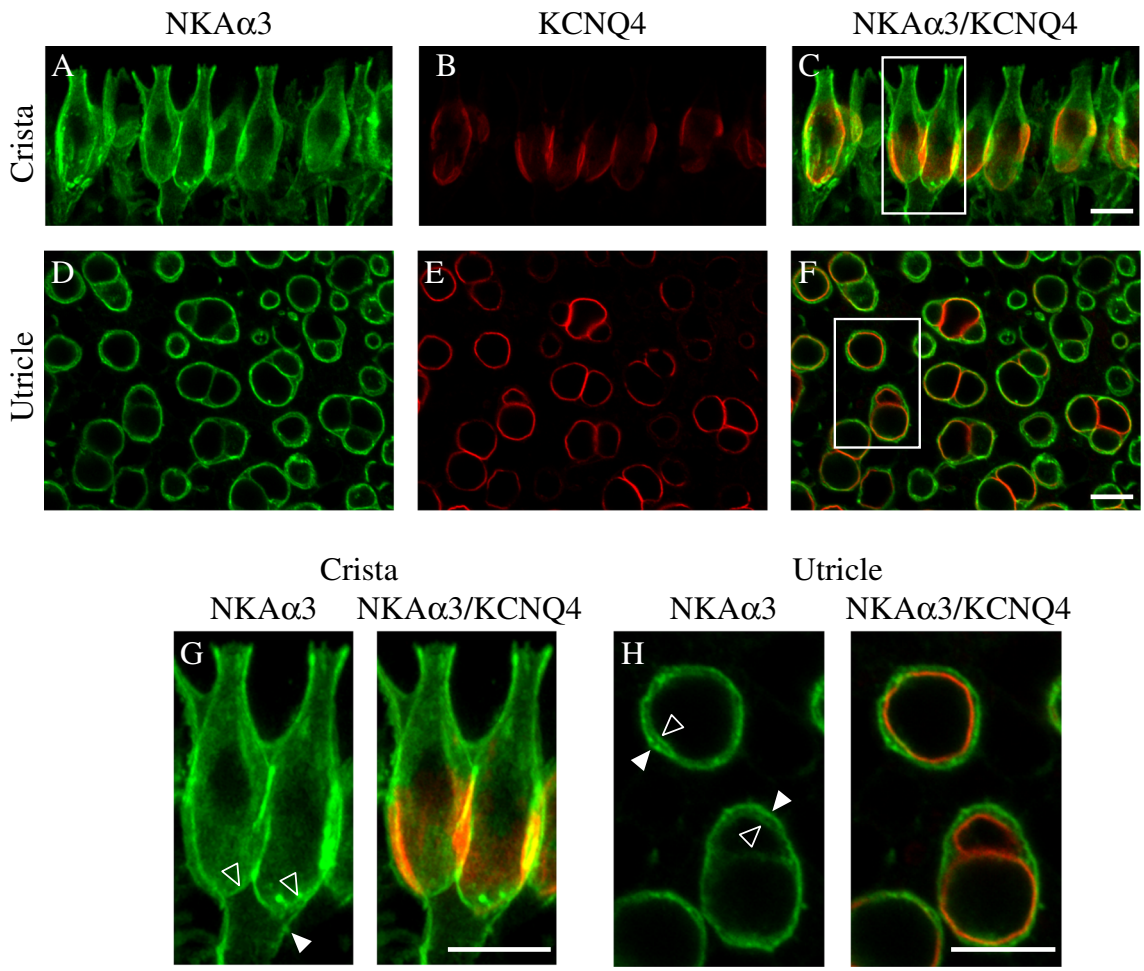

FIG. 4. NKAα3 is expressed throughout all calyx microdomains. High magnification micrographs of the central region of the horizontal crista (**A–C**) and striolar region of the utricle (**D–F**) double immunolabeled with a mouse monoclonal anti-NKAα3 (*green*, **A**, **D**, and **G** and **H**) and rabbit polyclonal anti- K_V7.4 (*red*, **B**, **E**, **G**, and **H**) to identify the molecular microdomains (Lysakowski et al. 2011) expressing the NKAα3. These micrographs reveal NKAα3 immunoreactivity colocalized with the K_V7.4-positive deep calyx inner face termed Domain 1 (**C**, **F**). **G**, **H** Higher magnification micrographs of the boxes in **C** and **F**. Vertically oriented calyces visible in the preparation of the crista (**G**) show that NKAα3 immunoreactivity additionally extends into Domain 2, the apical part of the calyx, as well as Domain 3, the basolateral calyx and axon segment. Similar patterns of immunoreactivity were observed in high magnification views of the anterior crista (data not shown). Higher magnification micrographs of the horizontally oriented calyces visible in the preparation of the utricle (**H**) show that NKAα3 immunoreactivity colocalizes with the K_V7.4-positive calyx inner face but is additionally expressed in the outer basolateral calyx membrane (**H**). Micrographs represent projections through the minimal number of optical sections required to completely visualize the hair cells and their afferent terminals (**A–C** and **G**) or single optical sections (**D–F** and **H**). Where clearly resolved, the inner-face (*open arrowhead*) and outer-face (*closed arrowhead*) calyx membranes are indicated. Scale *bars* measure 10 μm.

single optical sections from the striolar region of the utricle immunolabeled with a monoclonal antibody against NKAα3 (green, Fig. 6) and either a rabbit polyclonal antibody against GluA2/3 (red, Fig. 6A–C) or a goat polyclonal antibody against EAAT5 (red, Fig. 6D–F). GluA2/3 immunoreactivity was observed as puncta (Fig. 6B, C) localized to NKAα3-immunoreactive afferent calyces (Fig. 6A, C). EAAT5 immunoreactivity (Fig. 6E) showed overlapping distribution with NKAα3 immunoreactivity (Fig. 6D, F) throughout the afferent calyces.

A previous study of EAAT5 expression in mouse vestibular hair cells and calyx endings reported expression of EAAT5 in type I and type II hair cells as well as the calyx inner face (Dalet et al. 2012). Using one of the EAAT5 antibodies used in that study, we also observed immunoreactivity in the calyx inner face, but, in contrast to the previous report, labeling of the calyx outer face was observed, and labeling of type II hair cells was not observed. To examine whether differences in age (3 weeks in our study versus 3–5 weeks in the previous study) were respon-

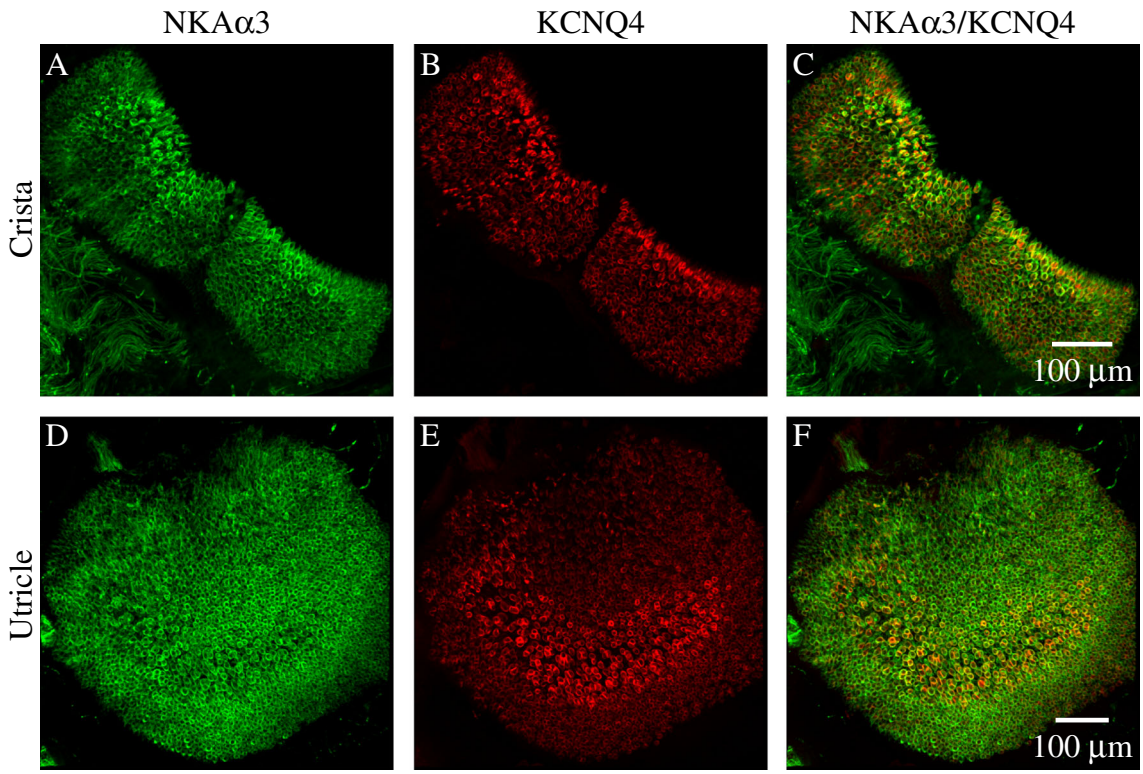

FIG. 5. NKAα3 is distributed uniformly throughout the vestibular sensory epithelia. Low magnification micrographs of the complete anterior crista (**A–C**) and utricle (**D–F**) double-immunolabeled with a mouse monoclonal anti-NKAα3 (*green,* **A** and **D**) and rabbit polyclonal anti-K_V7.4 (*red,* **B** and **E**). NKAα3 immunoreactivity is uniformly distributed throughout the sensory epithelia in contrast to the more conspicuous central-zone (**C**) and striolar (**F**) enrichment of K_V7.4 immunoreactivity. Similar patterns of immunoreactivity were observed in low magnification views of the horizontal crista (data not shown). Micrographs represent projections through the minimal number of optical sections required to completely visualize the sensory epithelia.

sible for the differences in expression, we also examined EAAT5 expression in 5-week-old rats (data not shown). Again, we observed immunolabeling in the calyx inner face and outer face and not in type II hair cells. Other differences such as the species (rat versus mouse) or specimen preparation (whole mounts versus sections) are possible factors accounting for the differences in observed expression. Nonetheless, both studies localize EAAT5 to the NKAα3-expressing calyx inner face.

The NKAα3 Subunit Is Not Expressed in Efferent Terminals

To examine expression of NKAα3 within the efferent terminals contacting the afferent terminals and type II hair cells, we triple immunolabeled preparations with a monoclonal (IgG1) antibody against NKAα3 (green, Fig. 7), a rabbit polyclonal antibody against synapsin (red, Fig. 7) to label efferent terminals (Favre et al. 1986; Scarfone et al. 1988), and a monoclonal (IgG2A) antibody against the type III β-tubulin (TuJ, blue, Fig. 7) to label afferent terminals. Similar to previous reports (Favre et al. 1986; Scarfone et al. 1988), we observed synapsin immunoreactivity colocalized with TuJ immunoreactivity in the necks of some calyx endings (data not shown). We also observed synapsin immunoreactivity at the depth in the epithelium where efferent terminals contact afferent terminals and type II hair cells. Relative to staining in the hair cell neck, the more basal synapsin immunoreactivity was more intense and more punctate, and did not colocalize with TuJ immunoreactivity, consistent with TuJ being a selective marker for afferent terminals. It is likely that the synapsin-positive, TuJ-negative terminals are efferent. (In the micrographs of Fig. 7A–C, fluorescence intensity was optimized to show the intense basal synapsin immunoreactivity, such that the less intense staining in the necks of the calyces was not visible.)

In the central region of the horizontal crista, projections through a z-stack of confocal sections spanning a single layer of sensory hair cells and their afferent terminals reveal NKAα3 immunoreactivity (Fig. 7A, C) completely surrounding the TuJ staining inside afferent calyces and bouton endings (Fig. 7C),

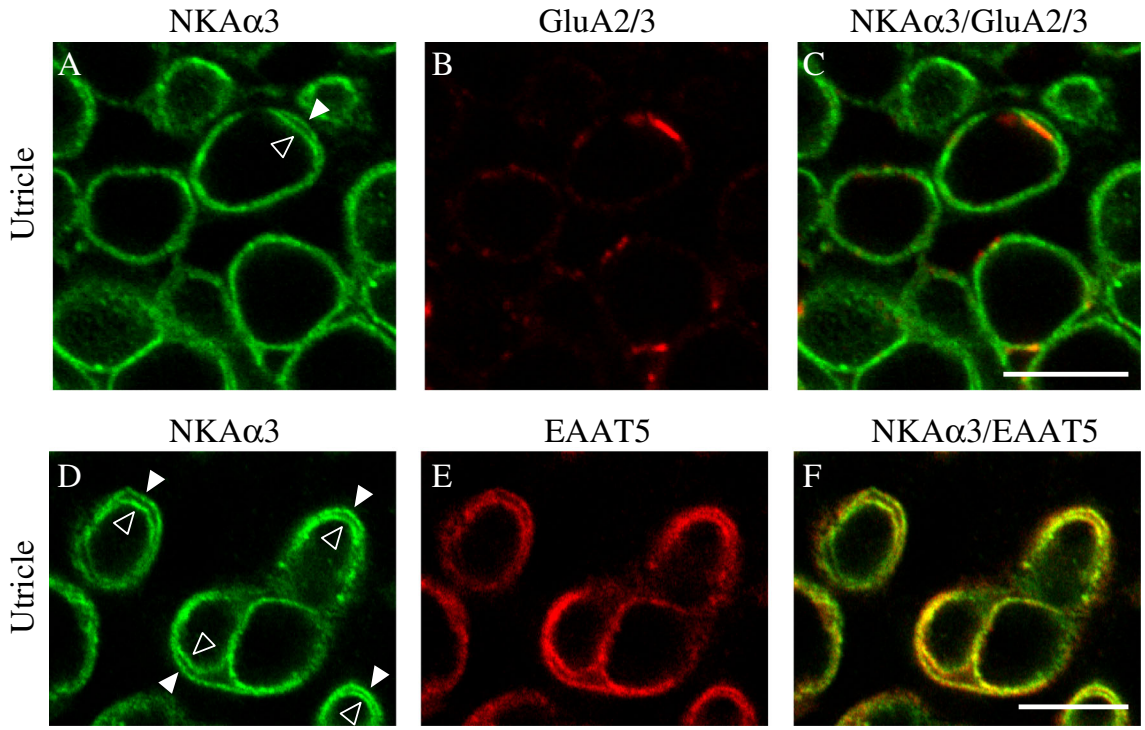

FIG. 6. NKAα3 is colocalized with glutamate receptors and transporters. High-magnification micrographs of the striolar region of the utricle double immunolabeled with a mouse monoclonal anti-NKAα3 (*green*, **A** and **D**) and either rabbit polyclonal anti-GluA2/3 (*red*, **B**) or goat polyclonal anti-EAAT5 (*red*, **E**) reveal NKAα3 immunoreactivity colocalized with GluA2/3-positive puncta (GluA2/3) on the calyx inner face (**C**) and EAAT5 immunoreactivity present on both the calyceal inner face and also the outer membrane (**F**). Similar patterns of immunoreactivity were observed in high magnification views of the anterior and horizontal cristae (data not shown). Micrographs represent single optical sections to better examine colocalization. Where clearly resolved, the inner (*open arrowhead*) and outer (*closed arrowhead*) calyx membranes are indicated (**A**, **D**). Scale *bars* measure 10 μm.

consistent with the expected membrane localization of transporters and cytosolic localization of intermediate filaments. In contrast, there was no NKAα3 immunoreactivity associated with synapsin-positive efferent terminals (Fig. 7B, C). Higher magnifications of the boxed regions in Figure 7C show synapsin-positive efferent terminals that lack NKAα3 immunoreactivity, on an afferent calyx (Fig. 7D; marked with closed arrowheads) and efferent terminals on afferent boutons (Fig. 7E; marked with closed arrowheads). Instead, NKAα3 immunoreactivity was exclusively associated with TuJ-positive afferent terminals (Fig. 7D, E; marked with open arrowheads in E). Similar patterns of immunoreactivity were observed in preparations of the anterior crista (data not shown). Examination of efferent terminals in single optical sections from the striolar region of the utricle show NKAα3 immunoreactivity (Fig. 7F, G) completely enclosing TuJ-positive afferent terminals, including both simple and complex afferent calyces (Fig. 7F) as well as bouton afferent terminals (Fig. 7G; marked with open arrowheads). In contrast, NKAα3 immunoreactivity does not enclose synapsin-positive efferent terminals on either afferent calyces (Fig. 7F; marked with closed arrowheads) or afferent bouton terminals (Fig. 7G; marked with closed arrowheads).

The NKAα1 Subunit Is Also Expressed in the Vestibular Sensory Epithelia

To determine if other subunits of NKAα are also expressed in the vestibular sensory epithelia, we immunolabeled preparations with various antibodies against NKAα1 and NKAα2. No immunoreactivity was detected for either of two antibodies used against NKAα2 (data not shown). We did not examine the expression of NKAα4, a subunit found exclusively in male gonadal tissues (Blanco et al. 2000). Similar patterns of immunoreactivity in the vestibular sensory epithelia were seen when immunostaining with either of two monoclonal (both IgG1) antibodies against NKAα1 (data from single immunolabeling experiments not shown). To localize NKAα1 immunoreactivity to particular structures within the vestibular sensory epithelia, we double-immunolabeled prepara-

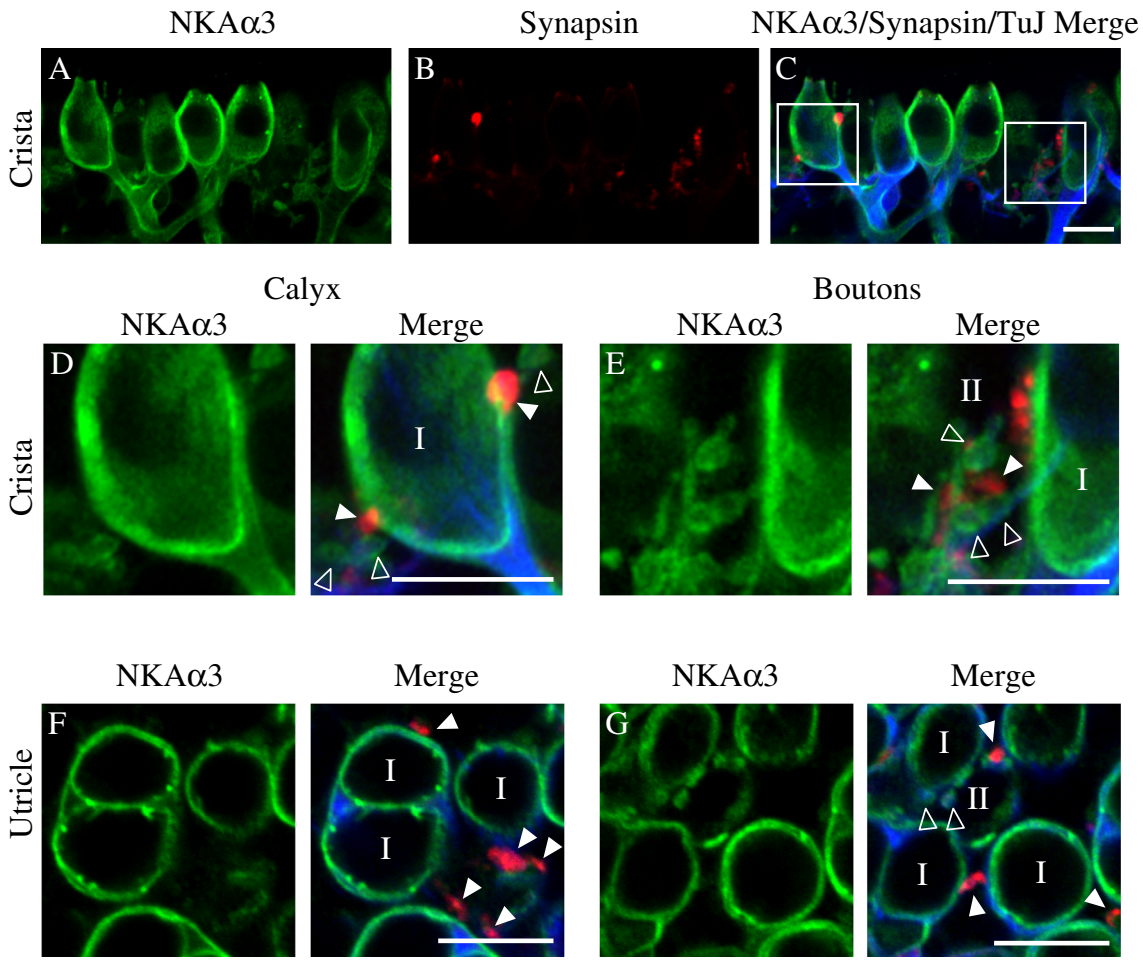

FIG. 7. NKAα3 is not expressed in the vestibular efferent terminals. **A–C** High-magnification micrographs of the central region of the anterior crista triple-immunolabeled with a mouse monoclonal (IgG1) anti-NKAα3 (*green*, **A**), rabbit polyclonal anti-synapsin (*red*, **B**), and mouse monoclonal (IgG2A) anti-TuJ (*blue*, **C**) reveal NKAα3 immunoreactivity that does not surround synapsin-identified efferent terminals (**C**). **D**, **E** Higher magnification views of the *left* and *right boxed regions* in **C**, respectively, show NKAα3 immunoreactivity in TuJ-positive afferent fibers but not synapsin-positive efferent terminals. Similar patterns of immunoreactivity were observed in high magnification views of the horizontal crista (data not shown). **F**, **G** Higher-magnification micrographs of the calyces viewed in cross-section in the utricle also show NKAα3 immunoreactivity that completely surrounds TuJ-positive afferent fibers but not synapsin-positive efferent terminals (**F** and **G**). Micrographs represent projections through the minimal number of optical sections required to completely visualize the hair cells and their afferent and efferent terminals (**A–E**) or single optical sections (**F** and **G**) to better resolve anatomical relationships. *Open arrowheads* indicate TuJ-positive afferent bouton terminals. *Closed arrowheads* indicate synapsin-positive efferent terminals. Scale *bars* measure 10 μm.

tions with a monoclonal antibody (IgG1) against NKAα1 (green, Fig. 8) and a monoclonal (IgG2A) antibody against type III β-tubulin (TuJ, red, Fig. 8) to label afferent terminals. Examination of afferent calyces from single optical sections of either the horizontal crista (Fig. 8A–C) or the striolar region of the utricle (Fig. 8D–F) show NKAα1 immunoreactivity (Fig. 8A, C and D, F) that is localized predominantly between TuJ-positive afferent calyces and the type I hair cells and also with type II hair cells contacted by TuJ-positive afferent boutons (Fig. 8B, C and E, F). The observed pattern of NKAα1 immunoreactivity suggests that NKAα1 is localized to the cell membranes of both type I and type II hair cells. To further investigate the hair-cell-specific localization of NKAα1 immunoreactivity, we examined patterns of NKAα1 immunoreactivity in vestibular sensory epithelia from rats at 3 days of age (P3), an age when the afferent calyx terminals have not yet completely engulfed the sensory hair cells (Meza et al. 1996; Rüsch et al. 1998). Single optical sections of the striolar region of the utricle (Fig. 8G–J) show NKAα1 immunoreactivity (green, Fig. 8G, J) in the membranes of Myo6-positive hair cells devoid of TuJ-positive afferent endings (red, Fig. 8H, J). NKAα1 immunoreactivity is also present, but more faintly, on Myo6-negative cells (marked with

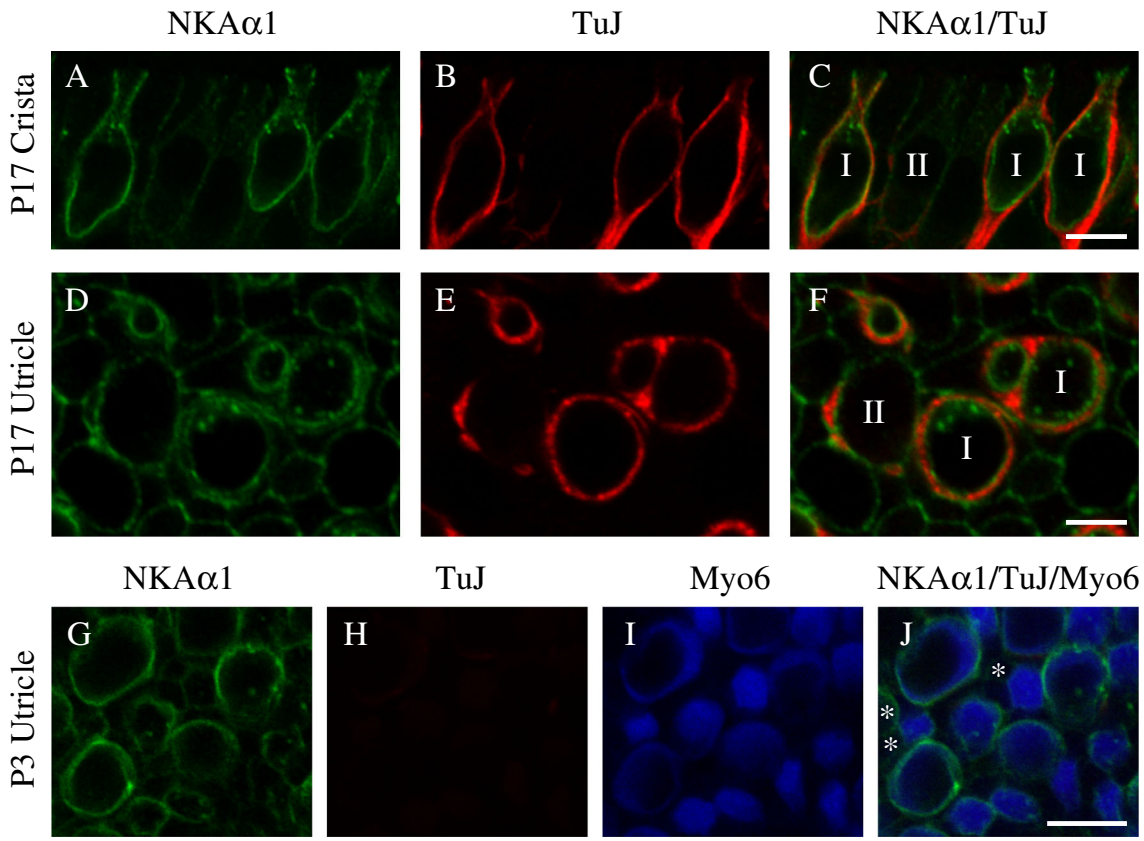

FIG. 8. NKAα1 is expressed in vestibular hair cells. High-magnification single optical sections of the central region of the horizontal crista (**A**–**C**) and striolar region of the utricle (**D**–**F**) double-immunolabeled with a mouse monoclonal anti-NKAα1 (*green,* **A** and **D**) and mouse monoclonal (IgG2A) anti-TuJ (*blue,* **C** and **F**). NKAα1 immunoreactivity is localized predominantly between TuJ-positive afferent calyces and type I hair cells and also on the membranes of type II hair cells contacted by TuJ-positive afferent boutons (**C** and **F**). **G**–**J** To examine the pattern of NKAα1 immunoreactivity at a developmental age preceding the appearance of afferent calyces, we examined high-magnification single optical sections of the striolar region of the utricle isolated from P3 rats. NKAα1 immunoreactivity (*green,* **G** and **J**) was seen around Myo6-positive hair cells (*blue,* **I** and **J**) in the absence of TuJ-positive afferent endings (*red,* **H** and **J**), consistent with its presence in the hair cell membrane. Fainter NKAα1 immunoreactivity was also detected around Myo6-negative support cells (marked with an *asterisk,* **I** and **J**). Similar patterns of immunoreactivity were observed in high-magnification single optical sections of the anterior and horizontal cristae isolated from P3 rats (data not shown). Scale *bars* measure 10 μm.

an asterisk, Fig. 8J), which are likely to be supporting cells although they may also be immature hair cells that do not yet express Myo6. Similar results were found in preparations of the crista from P3 rats (data not shown). We also examined P3 vestibular epithelia for NKAα3 immunoreactivity and found either no immunoreactivity or very weak immunoreactivity in the few nascent TuJ-positive afferent calyces evident at that age (data not shown).

The NKAα3 Subunit Is Expressed by the Second Postnatal Week and Stably into Adulthood

To further investigate the developmental expression of the NKAα3 subunit, we examined immunoreactivity in the early second postnatal week (P8), when young calyces have formed around type I hair cells (Meza et al. 1996), and at 6 weeks (P42), early adulthood. The pattern of NKAα3 immunoreactivity observed at P8 and at 6 weeks of age (Fig. 9) is similar to that observed between ages P17 and P25 (see Figs. 3 and 7). Importantly, at both the younger and later ages, NKAα3 immunoreactivity was present on both the calyx inner face and outer membranes and also afferent boutons. At 6 weeks of age, synapsin-positive efferent terminals targeting the base of the hair cells were devoid of NKAα3 immunoreactivity (Fig. 9D and F, closed arrowheads), indicating that the efferent terminals in mature preparations do not express the NKAα3 subunit (Fig. 9). At P8, there were some dimly labeled synapsin-positive efferent terminals at the base of the hair cells (Fig. 9B); at this age, efferent terminal innervation is thought to be immature (Dememes and Broca 1998). Interestingly, synapsin-immunoreactivity

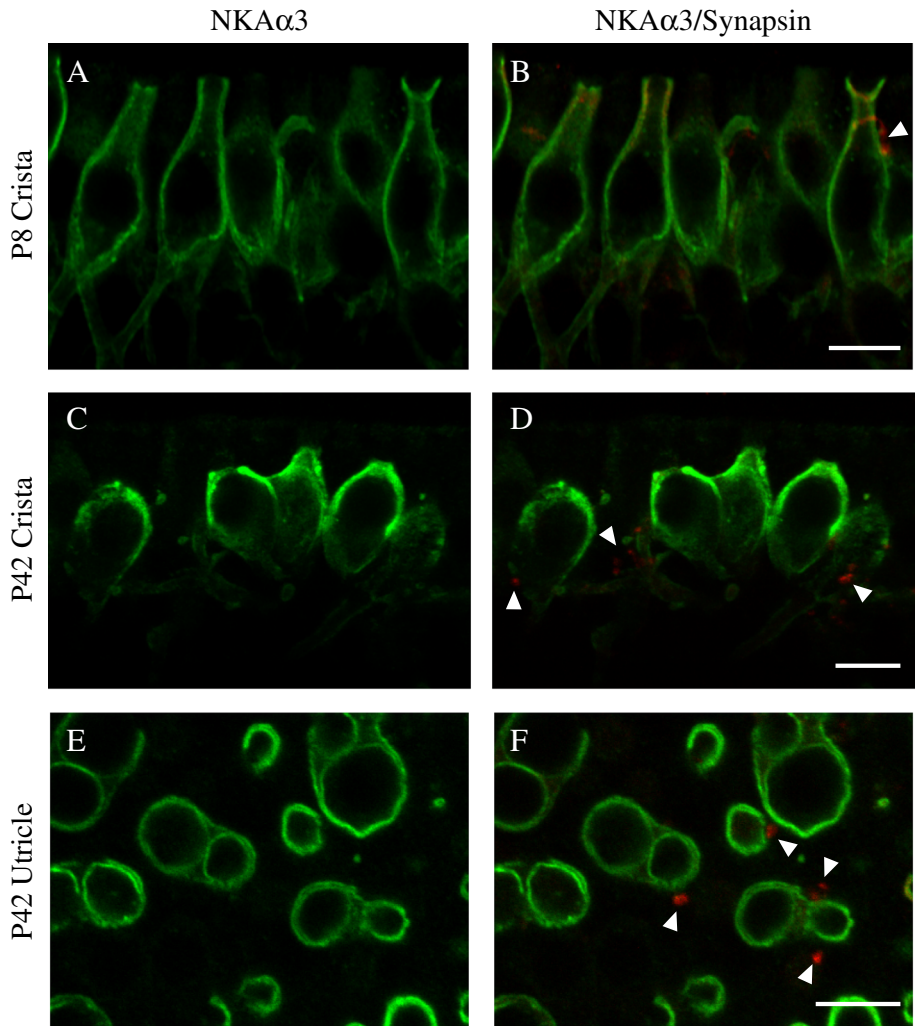

FIG. 9. NKAα3 is expressed by the second postnatal week and stably into adulthood. High-magnification single optical sections of the central region of the horizontal crista isolated from either P8 rats (**A**–**B**) or P42 (6 week) rats (**C**–**D**) and striolar region of the utricle isolated from P42 (6 week) rats (**E**–**F**) double-immunolabeled with a mouse monoclonal anti-NKAα3 (*green*, **A**–**F**) and rabbit polyclonal anti-synapsin (*red*, **B**, **D**, and **F**). NKAα3 immunoreactivity is present by the start of the second postnatal week (**A**) and continues into early adulthood (**C** and **E**). NKAα3 immunoreactivity is not associated with synapsin-positive efferent terminals (**B**, **D**, and **F**) at either age. Micrographs represent projections through the minimal number of optical sections required to completely visualize the hair cells and their afferent and efferent terminals (**A**–**D**) or single optical sections (**E** and **F**) to better resolve anatomical relationships. *Closed arrowheads* indicate synapsin-positive efferent terminals. Scale *bars* measure 10 μm.

was observed in the necks of the afferent calyces (Fig. 9B, closed arrowheads), as reported by Scarfone and colleagues (Favre et al. 1986; Scarfone et al. 1988).

DISCUSSION

To determine the contributions of the NKA to vestibular afferent signaling, we characterized the cellular and subcellular distribution of the NKA using immunofluorescence with subunit-specific antibodies against three NKAα subunits (1–3) and high-resolution confocal microscopy.

Within both canal and otolithic vestibular endorgans, we found expression of the NKAα3 subunit in all TuJ-identified afferent calyx and bouton endings. Within the afferent calyx endings, the NKAα3 subunit was expressed in all microdomains. Although we found no evidence that the NKAα3 subunit was missing from any afferent endings, future examination of NKAα3 expression along with other markers of afferent terminals could be performed. We also found no evidence for NKAα3 immunoreactivity in immunofluorescently identified efferent terminals. These observations are consistent with previous reports using isoform-specific immunocytochemistry in mouse (Schulte and Steel 1994), gerbil (McGuirt and

Schulte 1994), and rat (ten Cate et al. 1994), which localized NKAα3 immunoreactivity to the vestibular ganglion and calyx nerve endings surrounding type I hair cells. Localization to afferent boutons was previously observed with an isoform-nonspecific antibody against NKAα (Spicer et al. 1990). Earlier work did not address expression of NKAα in efferent endings.

We also found expression of the NKAα1 subunit in type I and type II hair cells but not the nerve endings. Previous reports on the distribution of NKAα1 are not consistent: Some studies, in agreement with our findings, have reported the absence of the NKAα1 subunit from the ganglion and nerve endings (McGuirt and Schulte 1994; Schulte and Steel 1994) while others have reported its presence (ten Cate et al. 1994). We found no evidence to indicate expression of the NKAα2 subunit in the vestibular sensory epithelia, again consistent with previous reports (Schulte and Steel 1994) but contradictory to another study (ten Cate et al. 1994). However, this latter study may have utilized an antibody against NKAα2 that was later determined to recognize NKAα3 (Schulte and Steel 1994). We also observed NKAα1 immunoreactivity in presumptive dark cells of the nonsensory region of the vestibular epithelia (data not shown) as has been well established (Wangemann 2002).

The patterns of NKAα3 and α1 immunoreactivity in the vestibular sensory epithelia suggest localization of NKAα3 to the afferent endings and localization of NKAα1 to the sensory hair cells and perhaps also the afferent calyces. Together with the established neuronal localization of the NKAα3 subunit in other tissues (Dobretsov and Stimers 2005), our observations that NKAα3 immunoreactivity completely envelopes TuJ-positive afferent terminals and colocalizes with the K_V7.4-positive calyx inner face convincingly localize NKAα3 to afferent terminals. Furthermore, the lack of NKAα3 immunoreactivity associated with the type II hair cell bodies and at ages preceding the developmental appearance of calyx endings are consistent with the absence of NKAα3 from the vestibular hair cells. This conclusion is in agreement with previous in situ hybridization experiments that found NKAα3 mRNA only in the neurons of the vestibular ganglion and not in the vestibular sensory epithelia (Fina and Ryan 1994). Similarly, NKAα1 immunoreactivity in the membranes of mature type II hair cells and of all hair cells before the developmental appearance of calyx endings (Fig. 8) indicates that vestibular hair cells express the NKAα1 subunit but does not rule out additional expression in the inner face of the afferent endings. Previous in situ hybridization experiments report NKAα1 mRNA in both the vestibular ganglion and the vestibular sensory epithelia (Fina and Ryan 1994), suggesting that NKAα1 is expressed by both the vestibular hair cells and the vestibular afferent neurons. Future characterization using immuno-electron microscopy and electrophysiology will be necessary to resolve definitively the distribution of the NKAα3 and α1 subunits, especially in the closely apposed membranes of the calyx inner face and type I hair cell.

Localization of the NKAα3 subunit to afferent endings likely shapes vestibular afferent signaling in a variety of ways. In both bouton and calyx terminals, NKAα3 no doubt regulates Na^+ and K^+ concentration gradients and membrane hyperpolarization essential to action potential generation. Biophysical characteristics of NKAα3 (Dobretsov and Stimers 2005), including its lack of inhibition at hyperpolarized potentials, relatively low affinity for intracellular Na^+, and relatively high affinity for ATP, make this subunit particularly suited to sustain the high firing rates typical of vestibular afferents (reviewed in Eatock and Songer 2011), which would be expected to cause prolonged depolarization, increase intracellular Na^+, and deplete intracellular ATP in the terminal. Moreover, in both calyx and bouton afferent endings, NKAα3 directly shapes synaptic transmission by maintaining the Na^+ concentration gradients necessary for Na^+-permeating AMPA-type glutamate receptors (GluAs) to mediate postsynaptic depolarization. Indeed, we observed colocalization of GluA2/3-containing AMPA receptors and NKAα3 in afferent terminals (Fig. 7). Interestingly, ouabain-induced inhibition of NKAα leads to GluA-dependent, rapid, and specific internalization and degradation of surface GluAs in cultured cortical neurons (Zhang et al. 2009), suggesting a novel, NKAα-mediated mechanism regulating Na^+ influx and GluA expression that could also occur in the inner ear.

The NKAα3 subunit may additionally shape afferent signaling in calyx terminals because of the unique morphology of these afferent endings. Firstly, the envelopment of the type I hair cell by the afferent calyx precludes glutamate uptake by supporting cells and necessitates mechanisms of glutamate clearance localized directly to the type I hair cell and/or calyx terminal. Indeed, recent work provides evidence that the glutamate transporter EAAT5 is expressed in calyx endings (Dalet et al. 2012). Like other glutamate transporters, EAAT5 relies at least indirectly on NKAs to generate the ion gradients necessary for the Na^+-dependent transport of glutamate (Beart and O'Shea 2007). Glutamate uptake is known to decrease when the inwardly directed Na^+ concentration gradient decreases (Zerangue and Kavanaugh 1996). Moreover, in the rat cerebellum, NKAαs and glutamate transporters form "macromolecular complexes" that are both physically and functionally coupled to regulate glutamate transport and consequently glutamatergic synaptic transmission (Rose et al. 2009; Sheean et al. 2013). Our observed colocalization of

NKAα3 and EAAT5 is not unexpected given the dependence of EAAT5 on Na^+ concentration gradients. Considering also the Na^+-dependence of GluAs, our observations suggest direct and previously unappreciated role of the NKAα3 subunit in shaping glutamatergic transmission at the hair cell-calyx afferent synapse. Finally, the presence of NKAα3 in the calyx inner face would also serve to clear K^+ that accumulates within the synaptic cleft because of the basolateral efflux of K^+ from the type I hair cell following mechanotransduction. K^+ accumulation would depolarize both pre- and postsynaptic elements and so affect excitability (Goldberg 1996), and depending on the kinetics of transport, NKAα3 would help to counter this depolarization. However, NKAα3 may not be sufficient to clear K^+ from the synaptic cleft: electrophysiological recordings provide experimental evidence for K^+ accumulation in intact preparations of the mouse crista (Lim et al. 2011; Contini et al. 2012). As these experiments were done at room temperature in excised preparations, it remains possible that clearance is more effective at body temperature in the intact animal.

We also observed interesting similarities and differences in NKAα3 and α1 subunit expression in the vestibular sensory epithelia compared with our previous examination of the auditory sensory epithelium (McLean et al. 2009). Similar to our observations in the auditory sensory epithelium, we found that vestibular afferent terminals express the NKAα3 subunit exclusively, and we found co-expression of NKAα subunits with glutamate transporters. Also similar to our observations in the auditory sensory epithelium, we observed punctate areas of increased NKAα3 immunoreactivity, suggestive of focal enrichment of the NKAα3, in some (but not all) afferent terminals. Within efferent endings, however, expression of NKAα subunits differs between the cochlea and vestibular organs. We reported NKAα3 expression by medial olivocochlear efferent endings but detected neither the NKAα3 nor NKAα1 in vestibular efferent endings, suggesting that they rely on alternative molecular mechanisms for Na^+ and K^+ homeostasis. Future identification of markers to identify efferent terminals specifically would help to substantiate this finding. NKAα expression also differs between cochlear and vestibular hair cells in that no NKAα expression was detected in cochlear hair cells. The expression of NKAα1 by vestibular hair cells and type I hair cells, in particular, may serve to support additional ion transport mechanisms imposed by the ensheathing calyx terminal.

Finally, we observed notable negative findings. Firstly, we found no difference in NKAα3 expression between the sensory epithelia of the utricle and the horizontal and anterior canals and no regional enrichment of the NKAα3 subunit within the vestibular sensory epithelia. This homogeneous distribution may result from the expression of NKAα3 by both calyx and bouton afferents but also suggests that the NKAα3 subunit might support a function common to all afferents rather than specifically contributing to regionally distributed regular versus irregular afferents or the encoding of different vestibular stimuli. Secondly, we observed no to weak NKAα3 immunoreactivity in nascent calyces in preparations from younger animals, suggesting a developmental lag in NKAα3 expression in afferent calyces. Reduced expression of NKAα3 in immature calyces would be expected to result in greater K^+ accumulation and might contribute to observed nonquantal transmission in type I afferent transmission in maturing preparations (Songer and Eatock 2013). Thirdly, we did not observe NKAα3 immunoreactivity in the support cells in either crista or macular sections or cells of the nonsensory region of the vestibular epithelia at either age (data not shown) also consistent with the expected neuronal localization of NKA α3.

In conclusion, our characterization of NKAα subunits in the vestibular sensory epithelia indicates that, in addition to their critical functions in endolymphatic homeostasis (Wangemann 2002), the NKAα1 and α3 subunits contribute to Na^+ and K^+ homeostasis and membrane polarization of the vestibular hair cells and afferent terminals, respectively, and are likely to directly affect afferent synaptic transmission by providing the Na^+ gradient required for glutamatergic neurotransmission.

ACKNOWLEDGMENTS

We thank Dr. Dwayne Simmons for the original suggestion to compare profile and cross-sectional views of the vestibular sensory epithelia. We gratefully acknowledge funds from UNC Wilmington to O. S. and S. J. P. and from NIDCD R01 DC0002290 and DC0012347 to R. A. E.

Conflict of Interest The authors declare that they have no conflict of interest.

REFERENCES

ARYSTARKHOVA E, SWEADNER KJ (1996) Isoform-specific monoclonal antibodies to Na,K-ATPase alpha subunits. Evidence for a tissue-specific post-translational modification of the alpha subunit. J Biol Chem 271:23407–23417

BEART PM, O'SHEA RD (2007) Transporters for L-glutamate: an update on their molecular pharmacology and pathological involvement. Br J Pharmacol 150:5–17

BEISEL KW, ROCHA-SANCHEZ SM, MORRIS KA, NIE L, FENG F, KACHAR B, YAMOAH EN, FRITZSCH B (2005) Differential expression of KCNQ4

in inner hair cells and sensory neurons is the basis of progressive high-frequency hearing loss. J Neurosci 25:9285–9293

BLANCO G, SANCHEZ G, MELTON RJ, TOURTELLOTTE WG, MERCER RW (2000) The alpha4 isoform of the Na,K-ATPase is expressed in the germ cells of the testes. J Histochem Cytochem 48:1023–1032

CONTINI D, ZAMPINI V, TAVAZZANI E, MAGISTRETTI J, RUSSO G, PRIGIONI I, MASETTO S (2012) Intercellular K(+) accumulation depolarizes type I vestibular hair cells and their associated afferent nerve calyx. Neuroscience 227:232–246

DALET A, BONSACQUET J, GABOYARD-NIAY S, CALIN-JAGEMAN I, CHIDAVAENZI RL, VENTEO S, DESMADRYL G, GOLDBERG JM, LYSAKOWSKI A, CHABBERT C (2012) Glutamate transporters EAAT4 and EAAT5 are expressed in vestibular hair cells and calyx endings. PLoS One 7:e46261

DEMEMES D, BROCA C (1998) Calcitonin gene-related peptide immunoreactivity in the rat efferent vestibular system during development. Brain Res Dev Brain Res 108:59–67

DESAI SS, ZEH C, LYSAKOWSKI A (2005A) Comparative morphology of rodent vestibular periphery. I. Saccular and utricular maculae. J Neurophysiol 93:251–266

DESAI SS, ALI H, LYSAKOWSKI A (2005B) Comparative morphology of rodent vestibular periphery. II. *Cristae ampullares*. J Neurophysiol 93:267–280

DESMADRYL G, DECHESNE CJ (1992) Calretinin immunoreactivity in chinchilla and guinea pig vestibular end organs characterizes the calyx unit subpopulation. Exp Brain Res 89:105–108

DOBRETSOV M, STIMERS JR (2005) Neuronal function and alpha3 isoform of the Na/K-ATPase. Front Biosci 10:2373–2396

EATOCK RA, SONGER JE (2011) Vestibular hair cells and afferents: two channels for head motion signals. Annu Rev Neurosci 34:501–534

FAVRE D, SCARFONE E, DI GIOIA G, DE CAMILLI P, DEMEMES D (1986) Presence of synapsin I in afferent and efferent nerve endings of vestibular sensory epithelia. Brain Res 384:379–382

FERNANDEZ C, BAIRD RA, GOLDBERG JM (1988) The vestibular nerve of the chinchilla. I. Peripheral innervation patterns in the horizontal and superior semicircular canals. J Neurophysiol 60:167–181

FERNANDEZ C, GOLDBERG JM, BAIRD RA (1990) The vestibular nerve of the chinchilla. III. Peripheral innervation patterns in the utricular macula. J Neurophysiol 63:767–780

FINA M, RYAN A (1994) Expression of mRNAs encoding alpha and beta subunit isoforms of Na,K-ATPase in the vestibular labyrinth and endolymphatic sac of the rat. Mol Cell Neurosci 5:604–613

GEERING K (2008) Functional roles of Na,K-ATPase subunits. Curr Opin Nephrol Hypertens 17:526–532

GOLDBERG JM (1996) Theoretical analysis of intercellular communication between the vestibular type I hair cell and its calyx ending. J Neurophysiol 76:1942–1957

HASSON T, GILLESPIE PG, GARCIA JA, MACDONALD RB, ZHAO Y, YEE AG, MOOSEKER MS, COREY DP (1997) Unconventional myosins in inner-ear sensory epithelia. J Cell Biol 137:1287–1307

HURLEY KM, GABOYARD S, ZHONG M, PRICE SD, WOOLTORTON JR, LYSAKOWSKI A, EATOCK RA (2006) M-like K + currents in type I hair cells and calyx afferent endings of the developing rat utricle. J Neurosci 26:10253–10269

ICHIMIYA I, ADAMS JC, KIMURA RS (1994) Immunolocalization of Na+, K(+)-ATPase, Ca(++)-ATPase, calcium-binding proteins, and carbonic anhydrase in the guinea pig inner ear. Acta Otolaryngol 114:167–176

LEONARD RB, KEVETTER GA (2002) Molecular probes of the vestibular nerve. I. Peripheral termination patterns of calretinin, calbindin and peripherin containing fibers. Brain Res 928:8–17

LIM R, KINDIG AE, DONNE SW, CALLISTER RJ, BRICHTA AM (2011) Potassium accumulation between type I hair cells and calyx terminals in mouse crista. Exp Brain Res 210:607–621

LYSAKOWSKI A, GABOYARD-NIAY S, CALIN-JAGEMAN I, CHATLANI S, PRICE SD, EATOCK RA (2011) Molecular microdomains in a sensory terminal, the vestibular calyx ending. J Neurosci 31:10101–10114

MCGUIRT JP, SCHULTE BA (1994) Distribution of immunoreactive alpha- and beta-subunit isoforms of Na,K-ATPase in the gerbil inner ear. J Histochem Cytochem 42:843–853

MCLEAN WJ, SMITH KA, GLOWATZKI E, PYOTT SJ (2009) Distribution of the Na,K-ATPase alpha subunit in the rat spiral ganglion and organ of corti. J Assoc Res Otolaryngol 10:37–49

MEZA G, ACUNA D, GUTIERREZ A, MERCHAN JM, RUEDA J (1996) Development of vestibular function: biochemical, morphological and electronystagmographical assessment in the rat. Int J Dev Neurosci 14:507–513

PERRY B, JENSEN-SMITH HC, LUDUENA RF, HALLWORTH R (2003) Selective expression of beta tubulin isotypes in gerbil vestibular sensory epithelia and neurons. J Assoc Res Otolaryngol 4:329–338

PRESSLEY TA (1992) Phylogenetic conservation of isoform-specific regions within alpha-subunit of Na(+)-K(+)-ATPase. Am J Physiol 262:C743–751

ROCHA-SANCHEZ SM, MORRIS KA, KACHAR B, NICHOLS D, FRITZSCH B, BEISEL KW (2007) Developmental expression of Kcnq4 in vestibular neurons and neurosensory epithelia. Brain Res 1139:117–125

ROSE EM, KOO JC, ANTFLICK JE, AHMED SM, ANGERS S, HAMPSON DR (2009) Glutamate transporter coupling to Na,K-ATPase. J Neurosci 29:8143–8155

RÜSCH A, LYSAKOWSKI A, EATOCK RA (1998) Postnatal development of type I and type II hair cells in the mouse utricle: acquisition of voltage-gated conductances and differentiated morphology. J Neurosci 18:7487–7501

SCARFONE E, DEMEMES D, JAHN R, DE CAMILLI P, SANS A (1988) Secretory function of the vestibular nerve calyx suggested by presence of vesicles, synapsin I, and synaptophysin. J Neurosci 8:4640–4645

SCHULTE BA, STEEL KP (1994) Expression of alpha and beta subunit isoforms of Na,K-ATPase in the mouse inner ear and changes with mutations at the Wv or Sld loci. Hear Res 78:65–76

SHEEAN RK, LAU CL, SHIN YS, O'SHEA RD, BEART PM (2013) Links between l-glutamate transporters, Na(+)/K(+)-ATPase and cytoskeleton in astrocytes: evidence following inhibition with Rottlerin. Neuroscience 254:335–346

SONGER JE, EATOCK RA (2013) Tuning and timing in mammalian type I hair cells and calyceal synapses. J Neurosci 33:3706–3724

SPICER SS, SCHULTE BA, ADAMS JC (1990) Immunolocalization of Na+, K(+)-ATPase and carbonic anhydrase in the gerbil's vestibular system. Hear Res 43:205–217

SPITZMAUL G, TOLOSA L, WINKELMAN BH, HEIDENREICH M, FRENS MA, CHABBERT C, DE ZEEUW CI, JENTSCH TJ (2013) Vestibular role of KCNQ4 and KCNQ5 K+ channels revealed by mouse models. J Biol Chem 288:9334–9344

TEN CATE WJ, CURTIS LM, RAREY KE (1994) Na,K-ATPase alpha and beta subunit isoform distribution in the rat cochlear and vestibular tissues. Hear Res 75:151–160

WANGEMANN P (2002) K+ cycling and the endocochlear potential. Hear Res 165:1–9

ZERANGUE N, KAVANAUGH MP (1996) Flux coupling in a neuronal glutamate transporter. Nature 383:634–637

ZHANG D, HOU Q, WANG M, LIN A, JARZYLO L, NAVIS A, RAISSI A, LIU F, MAN HY (2009) Na,K-ATPase activity regulates AMPA receptor turnover through proteasome-mediated proteolysis. J Neurosci 29:4498–4511